JAAS

PAPER

View Article Online
View Journal | View Issue

Cite this: *J. Anal. At. Spectrom.*, 2015, **30**, 1913

Mg/Ca ratios measured by laser induced breakdown spectroscopy (LIBS): a new approach to decipher environmental conditions

A. García-Escárzaga,†[a] S. Moncayo,†[b] I. Gutiérrez-Zugasti,†[a] M. R. González-Morales,[a] J. Martín-Chivelet[c] and J. O. Cáceres*[b]

Received 8th May 2015
Accepted 15th June 2015

DOI: 10.1039/c5ja00168d

www.rsc.org/jaas

The potential application of Mg/Ca ratios in top shells of the mollusc species *Phorcus lineatus* (Da Costa, 1778) obtained by Laser Induced Breakdown Spectroscopy (LIBS) has been evaluated as an environmental proxy to reconstruct paleotemperatures and season of capture of molluscs for the first time. All samples were collected from the Cantabrian Sea (Spain). The results were compared with instrumental sea surface temperatures (SSTs) and with a known reliable proxy as the oxygen isotope ratio ($\delta^{18}O_{shell}$) which is mainly dependent on the SST, obtained from the same shells. Measurements were taken in two different biominerals of the shell (aragonite and calcite) resulting in a correlation between Mg/Ca ratios and SSTs of $R^2 = 0.43$ and 0.44, respectively. Mg/Ca ratios were also studied through a long sequence on three shells collected in autumn 2012. The results show variations in Mg/Ca ratios related to seasonal changes in the SST throughout the year and a good correlation between Mg/Ca ratios and $\delta^{18}O_{shell}$ in two shells ($R^2 = 0.70$ and 0.65, respectively).

1. Introduction

The reconstruction of the climatic and environmental variability in the past depended on the fundamental task of obtaining high-resolution climate and environmental proxies. As many of these proxies are based on geochemical parameters, this task requires application of efficient analytical techniques to the obtained adequate geological, paleontological, or archaeological records.[1] Biological remains from archaeological sites can provide not only valuable data for reconstructing the past climate but can also yield key information about human activities. Among these, mollusc remains are found in many archaeological sites, commonly as large accumulation of shells as a result of human activities.[2] These shells can be excellent archives of the environmental conditions that existed during the life of the organism (and changes through it, for example, due to seasonal patterns) as well as indicators of human behaviour (*e.g.*, season of capture of molluscs, subsistence strategies, *etc.*[3]).

Most advances in the paleoclimatological analysis of these shells are related to the study of stable isotope ratios, mainly $\delta^{18}O$, which provide information about the sea water temperature,[4–8] and much less attention has been paid to other geochemical data of high potential, such as the trace element ratios in the biogenic carbonate. This potential, which is determined by the influence of temperature on the incorporation of chemical elements into the calcium carbonate along the shell growth axis, is however masked by the difficulties in retrieving significant and accurate data from the shells (for example, from micrometric growth layers) and in interpreting the data, as trace element concentrations are also non-environmental factor dependent.

With the aim of progressing in this direction, this paper presents the study of Mg/Ca ratios in the shells of modern specimens of the mollusc *Phorcus lineatus*, a gastropod abundant in present-day coastal areas and in archaeological sites. The relationship between the Mg/Ca ratio of shell carbonate and the temperature of water has been previously explored for several mollusc species under both laboratory and natural conditions, with remarkably different results.

A strong correlation of Mg/Ca with temperature has been shown in experimental work on *Patella rustica* and *Patella caerulea*,[9] *Pecten maximus*[10] and *Pinna nobilis*.[11] However, the correlation is much weaker in the case of *Tridacna gigas*,[12] *Concholepas concholepas*,[13] *Protothaca staminea*,[14] and *Cassostrea virginica*[15] or almost none in *Mesodesma donacium*,[16] *Chione subrugosa*,[16] *Mytilus californianus*,[17] *Arctica islandica*[18–20] and *Protothaca thaca*.[21]

This paper evaluates, for the first time, the usage of Laser Induced Breakdown Spectroscopy (LIBS),[22,23] to obtain the

[a]*Prehistoric International Research Institute of Cantabria, University of Cantabria, 39005 Santander, Spain*

[b]*Department of Analytical Chemistry, Faculty of Chemistry, Complutense University, 28040 Madrid, Spain. E-mail: jcaceres@ucm.es; Fax: +34 91 3944329; Tel: +34 91 3944322*

[c]*Department of Stratigraphy, Faculty of Geological Sciences, Complutense University and IGEO Geosciences Institute (CSIC-UCM), 28040 Madrid, Spain*

† These authors have contributed equally.

Mg/Ca ratios in the shells of modern specimens of the mollusc *Phorcus lineatus*. This technique provides significant advantages over conventional methods: minimal or no sample preparation, analysis at atmospheric pressure, higher spatial resolution (μm range), minimally destructive analysis, and good sensitivity.[24,25] Previous studies used other analytical techniques such as inductively coupled plasma-atomic emission spectroscopy (ICP-AES),[10,11,26–28] ICP-mass spectroscopy (ICP-MS)[9,11,21] and laser ablation-ICP-MS.[12–14,16,18–21] These elemental techniques offer high sensitivity and low detection limits. However, all these techniques except LA-ICP-MS involve wet chemistry processes (dissolution of the sample) that require long sample preparation procedures and microgram order of sample. The LA-ICP-MS technique requires a small sample for its inspection due to the reduced size of the sample chamber, moreover the analytical cost is substantially more expensive than LIBS.

In this work, in order to evaluate the potential of Mg/Ca data in the shells of *Phorcus lineatus* to infer sea-water paleo-temperatures, a double approach has been accomplished. Firstly, we analysed the Mg/Ca ratio of the shell aperture of different specimens collected monthly from Langre beach (N Spain) throughout a complete year, in order to know the compositional changes through time and its possible correlation with the sea surface temperature. Secondly, we analysed the variations in Mg/Ca through growth transects in three single shells ("sequential analysis") with the aim of recognizing possible cyclic patterns in compositional data that could correspond with seasonal changes in the temperature.

In a previous study, the samples used in this work were analysed for oxygen stable isotopes for evaluating the usage of the $\delta^{18}O_{shell}$ as a paleo-thermometer.[8] That study showed that the aragonite of *P. lineatus* grows under conditions of (or very close to) isotopic equilibrium of oxygen and that the water temperature can thus be inferred from the $\delta^{18}O_{shell}$ if the oxygen isotopic composition of water is known or can be estimated. These results are incorporated in this paper for comparison and calibration with the Mg/Ca data.

2. Materials and methods

2.1 Samples

Modern specimens of *P. lineatus* were collected periodically from October 2011 to October 2012 from Langre beach (Fig. 1) in the province of Cantabria, Spain. This mollusc lives up to 10 years and its top shell reaches 35 mm in length with an annual growth rate range of 15 to 26 mm (measured along the centre of the whorl),[29,30] allowing them to be analysed along the growth axis covering at least one year. A total of 47 shells were analysed. Table 1 gives the date of collection, SST provided by the Oceanographic Centre of Santander and the sample ID.

For cleaning the samples, all the shells were submerged in H_2O_2 (30%) and H_2O deionized (70%) solution for 48 hours, they were dried at ambient temperature, then cleaned in an ultrasonic bath for five minutes and finally dried at ambient temperature again.

The microstructure of *P. lineatus* has been studied in previous studies using scanning electron microscopy (SEM) and X-ray diffraction (XRD),[31] showing that they have an outer calcite layer and an inner aragonite layer. Fig. 2A and B show the morphology of *P. lineatus* and petrographic microscope images of a top shell microstructure: periostracum coating, prismatic and foliated calcite and aragonite.

2.2 LIBS set-up

The LIBS technique and the methodology used in the present work together with the most significant experimental conditions have been previously described.[32] Briefly, experiments were performed by using a Q-switched Nd:YAG laser (Quantel,

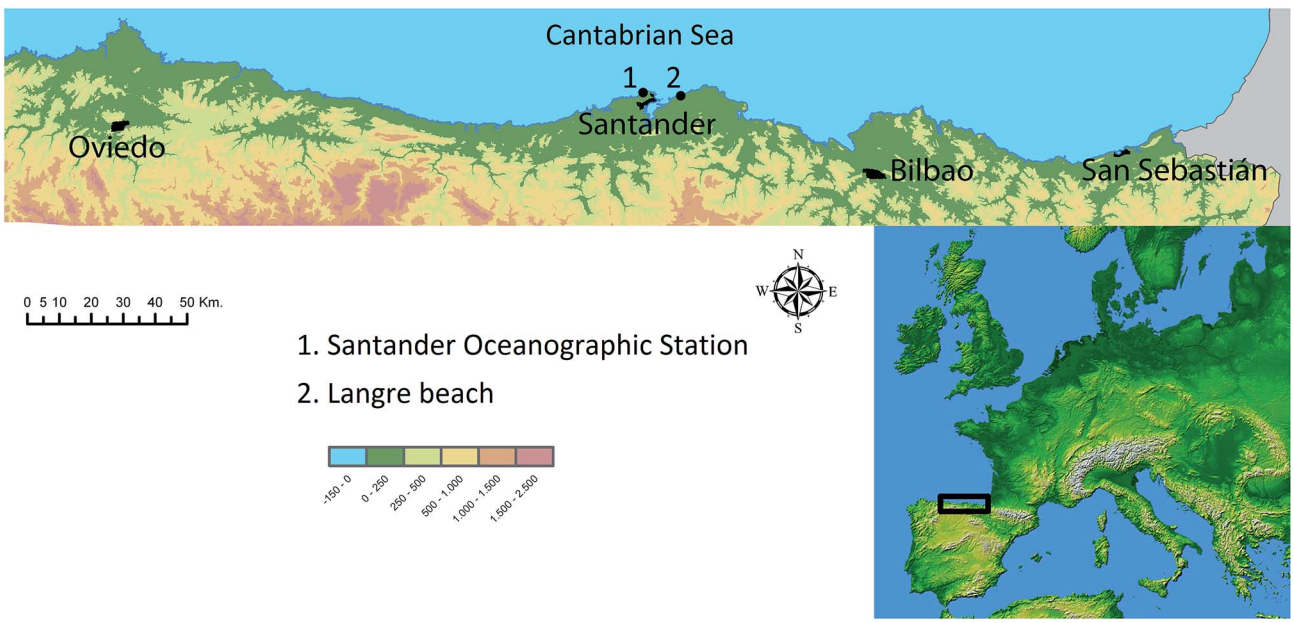

Fig. 1 Map of the Spanish Cantabrian Coast with the location of the Langre beach and Santander Oceanographic Station.

Table 1 Top shell collection and SST data

Sample ID	Collection date	Mean SST (°C) on the five days prior to shell collection
LANO-07	15/10/2011	17.9
LANO-08	15/10/2011	17.9
LANO-09	12/12/2011	16.6
LANO-10	12/12/2011	16.6
LANO-11	12/12/2011	16.6
LANO-12	25/11/2011	16.1
LANO-13	25/11/2011	16.1
LANO-14	25/11/2011	16.1
LANO-15	24/12/2011	13.6
LANO-16	24/12/2011	13.6
LANO-17	24/12/2011	13.6
LANO-18	12/01/2012	13.6
LANO-19	12/01/2012	13.6
LANO-20	12/01/2012	13.6
LANO-21	10/02/2012	11.8
LANO-22	10/02/2012	11.8
LANO-23	10/02/2012	11.8
LANO-24	23/02/2012	11.7
LANO-25	23/02/2012	11.7
LANO-26	23/02/2012	11.7
LANO-27	25/03/2012	12.8
LANO-28	25/03/2012	12.8
LANO-29	25/03/2012	12.8
LANO-30	22/04/2012	13.0
LANO-31	22/04/2012	13.0
LANO-32	22/04/2012	13.0
LANO-33	05/05/2012	13.8
LANO-34	05/05/2012	13.8
LANO-35	05/05/2012	13.8
LANO-36	03/06/2012	15.3
LANO-37	03/06/2012	15.3
LANO-38	03/06/2012	15.3
LANO-39	21/06/2012	17.5
LANO-40	21/06/2012	17.5
LANO-41	21/06/2012	17.5
LANO-42	22/07/2012	19.4
LANO-43	22/07/2012	19.4
LANO-44	22/07/2012	19.4
LANO-45	05/08/2012	21.0
LANO-46	05/08/2012	21.0
LANO-47	05/08/2012	21.0
LANO-48	02/09/2012	21.5
LANO-49	02/09/2012	21.5
LANO-50	02/09/2012	21.5
LANO-04	01/10/2012	19.1
LANO-05	01/10/2012	19.1
LANO-52	01/10/2012	19.1

Brio model) operating at 1064 nm, with a pulse duration of 4 ns full width at half maximum. The samples were placed directly over an *x*-*y*-*z* manual micrometric positionator with a 0.5 μm step to ensure that each laser pulse impinged on a fresh position. The laser beam was focused onto the sample surface with a 100 mm focal-distance lens, producing a spot of 100 μm in diameter. The laser fluence was fixed to 20 J cm^{-2} and the repetition rate was 1 Hz. Emission from the plasma was collected with a 4 mm aperture, with a 7 mm focus fused silica collimator placed at a distance of 3 cm from the sample, and

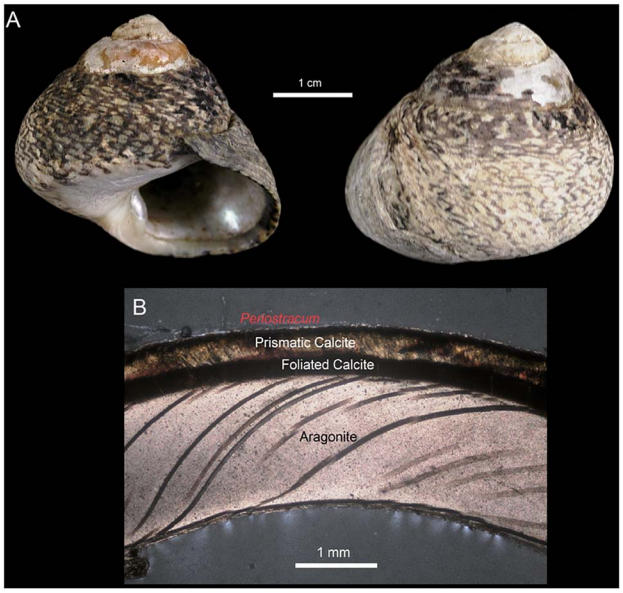

Fig. 2 *P. lineatus* specimens: (A) morphology of the *P. lineatus* top shell. (B) Cross-section showing different crystalline structures: aragonite, foliated and prismatic calcite and the organic periostracum coating.

then focused into an optical fiber (with a 1000 μm core diameter and 0.22 numerical aperture), which was coupled to the entrance of the spectrometer. The spectrometer system was a user-configured miniature single-fiber system (EPP2000, StellarNet, Tampa, FL, U.S.A.) with a gated CCD detector. A grating of 300 l mm^{-1} was selected; a spectral resolution of 0.5 nm was achieved with a 7 μm entrance slit. The spectral range used was from 200 to 1000 nm. The detector integration time was set to 1 ms. In order to prevent the detection of bremsstrahlung, the detector was triggered with a 5 μs delay time between the laser pulse and the acquired plasma radiation using a digital delay generator (Stanford model DG535).

2.3 LIBS analysis

For shell analysis, a Dremel microdrill model with a 2 mm drill bit was used for removing the outer layers (*i.e.* periostracum and calcite layer) when necessary. For LIBS analysis, Mg/Ca ratios

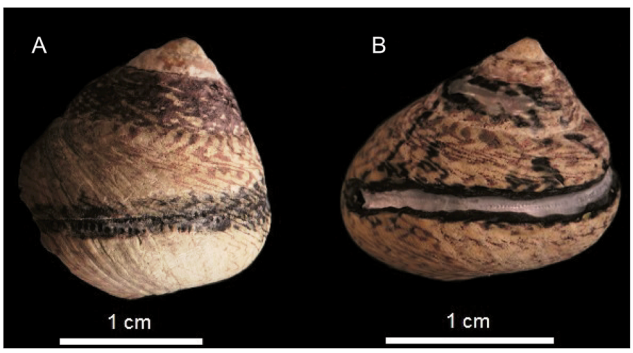

Fig. 3 Crater trace formed by laser shots in (A) calcite and (B) aragonite layers.

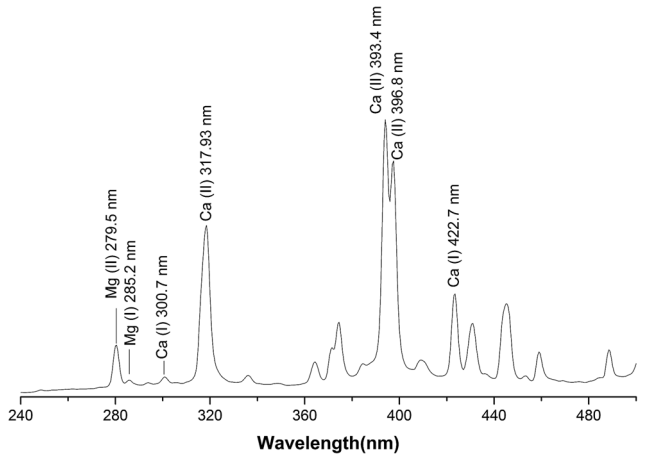

Fig. 4 LIBS spectrum of the *P. lineatus* sample.

were measured in two different biogenic carbonates present in this mollusc: prismatic calcite and aragonite.

Each LIBS spectrum was obtained by averaging 20 laser pulses at the same position. A relative standard deviation (RSD) of less than 5% was achieved. The sampling positions were separated by 200 μm covering at least 3.2 cm of shell growth taking approximately 160 LIBS spectra for each sample. The emission lines used for Mg(II) and Ca(I) were 279.55 nm and 422.67 nm, respectively because of their high signal to noise ratio and to avoid the saturation or even the interferences with other emission lines. Fig. 3 shows the crater trace formed by sequential laser shots in both calcite (A) and aragonite (B) layers along the growth of the shells.

3. Results and discussion

LIBS experiments were performed on 47 modern shells of *P. lineatus*. Fig. 4 shows a typical LIBS spectrum of the aragonite layer of the shell covering a range of 240.0 nm to 500.0 nm. The assignation of the emission lines from the main elements at their corresponding wavelengths was carried out based on the NIST atomic spectra database.[33] The most representative lines in nm were Mg(I) (285.2), Mg(II) (279.5), Ca(I) (300.7; 422.7) and Ca(II) (317.9; 393.4; 396.8). Due to the morphology of the sample (spiral) in order to keep the same focusing condition, each measurement along the mollusc growth was corrected by means of a *x-y-z* micrometric-positioner avoiding the defocusing effect and enhancing the reproducibility of the measurements.

3.1. Mg/Ca ratios from shell aperture samples

The annual correlation between the SST and the Mg/Ca ratios in aragonite and calcite layers obtained for 47 *P. lineatus* top shells is shown in Fig. 5A and B. Each value of the Mg/Ca ratio was

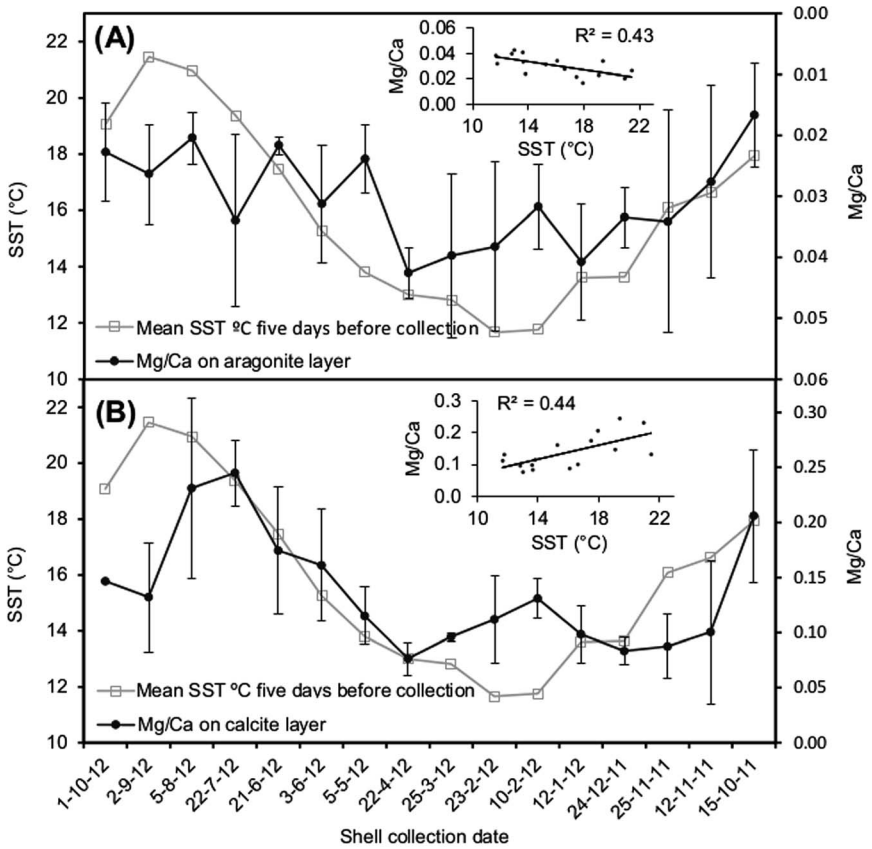

Fig. 5 Annual correlation between the SST and Mg/Ca ratio in the (A) aragonite layer and (B) calcite.

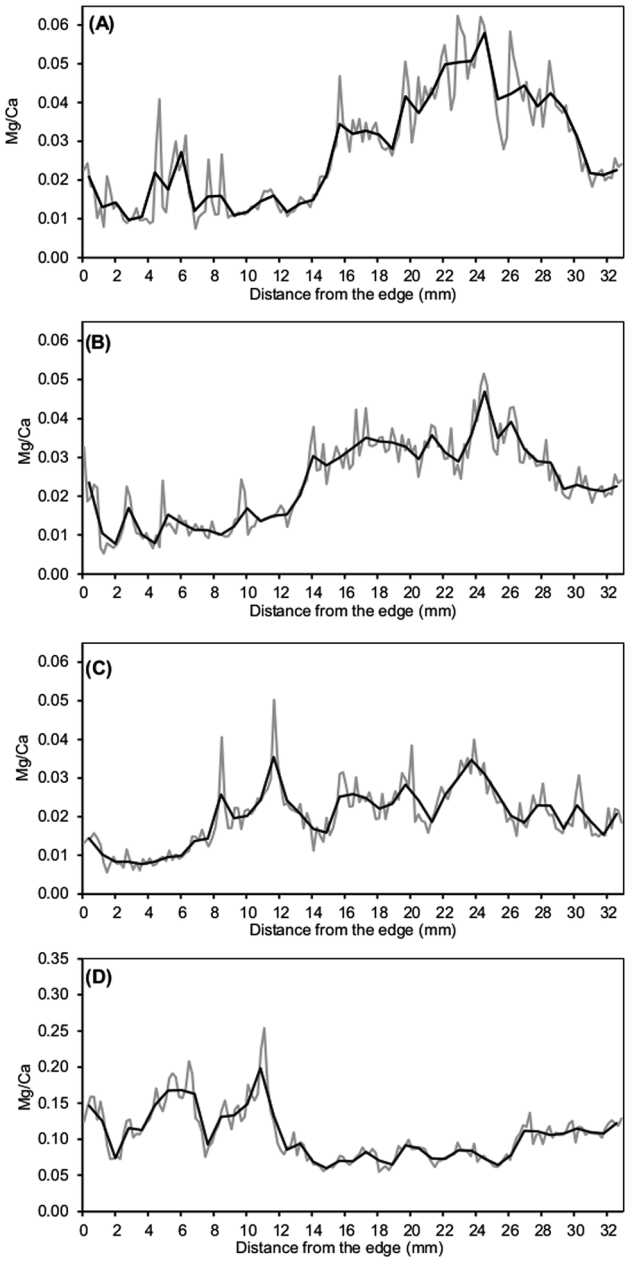

Fig. 6 Mg/Ca ratios along the growth direction in four top shells, the first two (A) LANO-4, (B) LANO-5 were measured in the aragonite layer and last one LANO-52 in both (C) aragonite and (D) calcite layers. Grey lines show the result obtained on each point measured and black lines show the average of four Mg/Ca values.

obtained by averaging the first four values of the shell aperture for three different shells collected on the same day. The error bars represent the relative standard deviation (RSD) between the shell specimens. The highest Mg/Ca ratio was found in the calcite layer, 0.319, whereas in the aragonite layer it was 0.06. This difference is attributed to the fact that calcite and magnesium carbonate have a hexagonal crystalline structure, and therefore solid solutions between these two phases occur frequently.[34] Moreover, the atomic radius of Ca and Mg is similar and Mg could be easily incorporated into the calcite

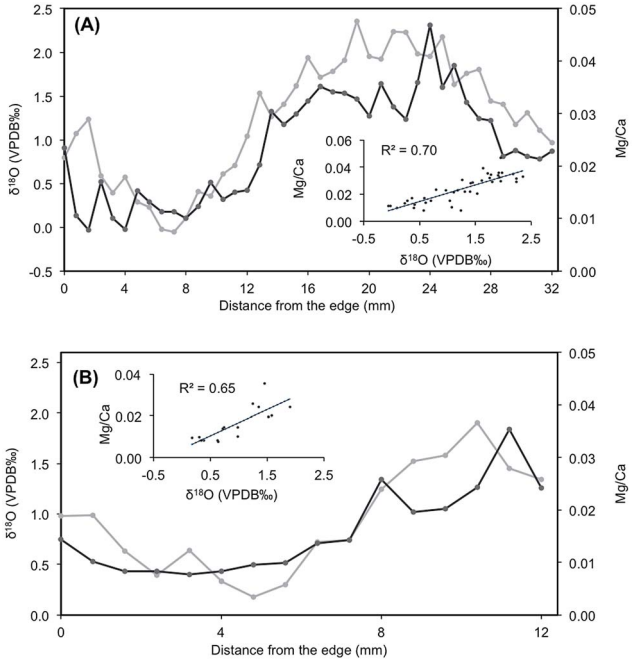

Fig. 7 Relationship between $\delta^{18}O_{shell}$ and Mg/Ca ratios in *P. lineatus* top shells along the growth axes. (A) LANO-5 (B) LANO-52.

structure. On the other hand, the aragonite layer has an orthorhombic crystalline structure, making the incorporation of Mg unfavourable.[35,36] The relationship between Mg/Ca ratios and the SST is inverse (Fig. 5A) in the aragonite layer whereas it is directly proportional in the calcite layer (Fig. 5B). Therefore, an increase in the Mg/Ca ratios measured in the calcite is observed in periods of high temperature, while measurements in the aragonite showed increased elemental ratios under colder conditions. A correlation coefficient (R^2) of 0.43 and 0.44 was obtained between Mg/Ca ratios for aragonite and calcite layers with SST, respectively. This correlation in the Mg/Ca ratios demonstrates that incorporation of magnesium into biogenic carbonates is not only influenced by temperature changes but also by other factors such as salinity, food quality and quantity and reproductive cycles, among others.[37] Nevertheless, the concentration of an element in a specific position on the growth axis is substantially homogeneous within a layer and thus no significant variations in the elemental ratios are observed with the depth of the crater. Furthermore, the high RSD values of 30.7% and 25.9% in aragonite and calcite respectively for different shells collected on the same day reflect the variability between specimens of the same species growing under the same environmental conditions, which indicates that the incorporation of trace elements is physiologically controlled by factors such as metabolism, kinetic effects, calcification rates, differences in crystal growth orientation and morphology.[11,26,27,38,39]

3.2. Mg/Ca ratios from sequential samples

Three top shells were analysed by LIBS along their growth axes considering at least one year. Mg/Ca ratios from LANO-4 and

LANO-5 shells were measured only on the aragonite layer, whereas LANO-52 was measured in both aragonite and prismatic calcite layers.

The sequence obtained from LANO-4, LANO-5 and LANO-52 aragonite samples (Fig. 6A–C) shows minimum values in the first 13–15 mm from the shell aperture, increasing quickly in the next 10–12 mm, and decreasing again. A similar trend was observed for all specimens collected on the same day. This sinusoidal pattern is related to seasonal changes in the SST throughout the year, with maximum values exhibiting lower temperatures. The sequence of LANO-52 from the prismatic calcite layer (Fig. 6D) had an inverse behaviour, with Mg/Ca increasing during warmer months and decreasing in winter. The results obtained in calcite and aragonite are in accordance with the expected trends and with results from shell aperture samples. The incorporation of Mg as an impurity into calcite is endothermic,[40] therefore more amount of this element is incorporated into the crystal at higher temperatures, as opposed to the aragonite layer.

Finally, isotope sequences from LANO-5 and LANO-52 in the aragonite layer were compared with Mg/Ca ratios.[8] The mean of four LIBS measurements of elemental ratios corresponded approximately to one isotope measurement. A high correlation value between Mg/Ca ratios and $\delta^{18}O_{shell}$ was found ($R^2 = 0.7$) in the case of LANO-5 (Fig. 7A), but not in the case of LANO-52, that presents a low correlation ($R^2 = 0.07$). Nonetheless, if we use only the last 12 mm of growth of LANO-52 (Fig. 7B), the correlation becomes significant ($R^2 = 0.65$). This anomaly, observed in the portions of growth after 12 mm in LANO-52, is difficult to explain, although can be mentioned that the elemental ratios are not only dependent on the SST. If we consider the correlation obtained from LANO-5 and the first middle part of LANO-52, the correlations presented in this paper are among the highest determination coefficients documented until date, since only Ferguson *et al.*[9] and Freitas *et al.*[10] published a higher correlation on limpets ($R^2 = 0.79$) and scallops ($R^2 = 0.77$), respectively.

4. Conclusions

The use of Mg/Ca ratios obtained using the LIBS technique in mollusc species as paleoclimatic proxy has been reported for the first time. The analyses of Mg/Ca ratios on *P. lineatus* using the LIBS technique provide successful results, showing the great potential of the technique for environmental analysis and as a marker of seasonality. Tracing past environmental conditions is crucial for many disciplines, such as palaeoclimatology, archaeology, palaeoceanography or palaeontology, and establishing the season of capture has important implications particularly for archaeological studies, since it is a key issue for the reconstruction of settlement patterns and subsistence strategies of hunter–fisher–gatherers.

The correlation coefficients between Mg/Ca ratios and $\delta^{18}O_{shell}$ suggest that the incorporation of trace elements into the calcium carbonate of *P. lineatus* is not only dependent on the environmental temperature, but also by other factors such as salinity, food quality and quantity, reproductive cycles and others, although the information obtained did not allow us to know the causes that are involved in the process of shell formation.

The feasibility of the LIBS technique as analytical methodology for the determination of climate patterns and their correlation with other techniques as $\delta^{18}O$ and finally with the temperature has pointed out LIBS as an analytical technique is appropriate to perform elemental analysis of mollusc shells. In addition, LIBS allows us to obtain results quickly and considerable cost reduction without the loss of archaeological materials. However, further work is needed to improve the correlation coefficients and determine the influence of other parameters on the incorporation of Mg into different allotropic forms of carbonate in the shell molluscs.

Acknowledgements

This research was performed as part of the project "The human response to the global climatic change in a littoral zone: the case of the transition to the Holocene in the Cantabrian coast (10000–5000 cal BC) (HAR2010-22115-C02-01)" funded by the Spanish Ministry of Economy and Competitiveness. Two of the authors AGE and IGZ were supported by a predoctoral grant from the University of Cantabria and a contract of the Juan de la Cierva programme funded by the Spanish Government, respectively. We must thank the Fishing Activity Service of the Cantabrian Government for the authorization to collect the modern *P. lineatus*, the Aquaculture Facility of Santander's Oceanographic Center for providing the information related to sea surface temperatures, José Ramón Mira Soto for his help measuring salinity and Adolfo Cobo García for his comments. The materials and resources were provided by the Instituto Internacional de Investigaciones Prehistóricas de Cantabria (IIIPC), the University of Cantabria and the Complutense University of Madrid.

References

1 I. Burton, B. Challenger, S. Huq, R. J. T. Klein and G. Yohe, *Adaptation to Climate Change in the Context of Sustainable Development and Equity, Chap 18*, IPCC Working Group II, Washington DC, USA, 2001.
2 M. Álvarez, I. Briz Godino, A. Balbo and M. Madella, *Quaternary Int.*, 2011, **239**, 1–7.
3 C. F. T. Andrus, *Quat. Sci. Rev.*, 2011, **30**, 2892–2905.
4 A. C. Colonese, S. Troelstra, P. Ziveri, F. Martini, D. Lo Vetro and S. Tommasini, *J. Archaeol. Sci.*, 2009, **36**, 1935–1944.
5 A. L. Prendergast, M. Azzopardi, T. C. O'Connell, C. Hunt, G. Barker and R. E. Stevens, *Chem. Geol.*, 2013, **345**, 77–86.
6 T. Wang, D. Surge and S. Mithen, *Palaeogeogr., Palaeoclimatol., Palaeoecol.*, 2012, **317–318**, 104–113.
7 M. A. Mannino, K. D. Thomas, M. J. Leng and H. J. Sloane, *Geo-Mar. Lett.*, 2008, **28**, 309–325.
8 I. Gutierez Zugasti, A. Garcia Escarzaga, J. Martin-Chivelet and M. R. Gonzalez-Morales, *Holocene*, 2015, **25**, 1002–1014.

9 J. E. Ferguson, G. M. Henderson, D. A. Fa, J. C. Finlayson and N. R. Charnley, *Earth Planet. Sci. Lett.*, 2011, **308**, 325–333.
10 P. S. Freitas, L. J. Clarke, H. Kennedy and C. A. Richardson, *Chem. Geol.*, 2012, **291**, 286–293.
11 P. Freitas, L. J. Clarke, H. Kennedy, C. Richardson and F. Abrantes, *Geochem., Geophys., Geosyst.*, 2005, **6**, 1–16.
12 M. Elliot, K. Welsh, C. Chilcott, M. McCulloch, J. Chappell and B. Ayling, *Palaeogeogr., Palaeoclimatol., Palaeoecol.*, 2009, **280**, 132–142.
13 C. E. Lazareth, N. Guzman, F. Poitrasson, F. Candaudap and L. Ortlieb, *Geochim. Cosmochim. Acta*, 2007, **71**, 5369–5383.
14 R. K. Takesue and A. van Geen, *Geochim. Cosmochim. Acta*, 2004, **68**, 3845–3861.
15 D. Surge and K. C. Lohmann, *J. Geophys. Res.: Biogeosci.*, 2008, **113**, G02001.
16 M. Carré, I. Bentaleb, O. Bruguier, E. Ordinola, N. T. Barrett and M. Fontugne, *Geochim. Cosmochim. Acta*, 2006, **70**, 4906–4920.
17 H. L. Ford, S. A. Schellenberg, B. J. Becker, D. L. Deutschman, K. A. Dyck and P. L. Koch, *Paleoceanography*, 2010, **25**, PA1203.
18 L. C. Foster, A. A. Finch, N. Allison, C. Andersson and L. J. Clarke, *Chem. Geol.*, 2008, **254**, 113–119.
19 B. R. Schöne, Z. Zhang, P. Radermacher, J. Thébault, D. E. Jacob, E. V. Nunn and A.-F. Maurer, *Palaeogeogr., Palaeoclimatol., Palaeoecol.*, 2011, **302**, 52–64.
20 H. Toland, B. Perkins, N. Pearce, F. Keenan and M. J. Leng, *J. Anal. At. Spectrom.*, 2000, **15**, 1143–1148.
21 C. E. Lazareth, F. Le Cornec, F. Candaudap and R. Freydier, *Palaeogeogr., Palaeoclimatol., Palaeoecol.*, 2013, **373**, 39–49.
22 D. A. Cremers and L. J. Radziemski, *Handbook of laser-induced breakdown spectroscopy*, Wiley-Blackwell, Oxford, UK, 2nd edn, 2013.
23 S. Musazzi and U. Perini, *Laser-Induced Breakdown Spectroscopy – Theory and Applications*, Springer, Milan, Italy, 2014, vol. 182.
24 F. J. Fortes, I. Vadillo, H. Stoll, M. Jiménez-Sánchez, A. Moreno and J. J. Laserna, *J. Anal. At. Spectrom.*, 2012, **27**, 868–873.
25 A. Marín-Roldán, J. A. Cruz, J. Martín-Chivelet, M. J. Turrero, A. I. Ortega and J. O. Caceres, *J. Appl. Laser Spectrosc.*, 2014, **1**, 7–12.
26 P. S. Freitas, L. J. Clarke, H. Kennedy, C. A. Richardson and F. Abrantes, *Geochim. Cosmochim. Acta*, 2006, **70**, 5119–5133.
27 P. S. Freitas, L. J. Clarke, H. A. Kennedy and C. A. Richardson, *Biogeosciences*, 2008, **5**, 1245–1258.
28 P. S. Freitas, L. J. Clarke, H. Kennedy and C. A. Richardson, *Biogeosciences*, 2009, **6**, 1209–1227.
29 J. M. Gaillard, *Aspects qualitatifs et quantitatifs de la croissance de la coquille de quelques espèces de Mollusques Prosobranches en fonction de la latitude et des conditions écologiques*, Mémoires du meséum National d'Historie Naturalle, Éditions du Muséum, Lahure-Fr, 1965, **38**, 1–55.
30 M. B. Regis, *J. Molluscan Stud.*, 1972, **3**, 259–267.
31 M. A. Mannino, B. F. Spiro and K. D. Thomas, *J. Archaeol. Sci.*, 2003, **30**, 667–679.
32 S. Moncayo, S. Manzoor, T. Ugidos, F. Navarro-Villoslada and J. O. Caceres, *Spectrochim. Acta, Part B*, 2014, **101**, 21–25.
33 NIST Atomic Spectra Database, US Department of Commerce, http://physics.nist.gov/PhysRefData/ASD/lines_form.html, Cited June 5 2015.
34 R. M. Hazen, R. T. Downs, A. P. Jones and L. Kah, *Rev. Mineral. Geochem.*, 2013, **75**, 7–46.
35 A. A. Finch and N. Allison, *Geophys. Res. Lett.*, 2008, **35**, L08704.
36 O. Branson, S. A. T. Redfern, T. Tyliszczak, A. Sadekov, G. Langer, K. Kimoto and H. Elderfield, *Earth Planet. Sci. Lett.*, 2013, **383**, 134–141.
37 H. Toland, B. Perkins, N. Pearce, F. Keenan and M. J. Leng, *J. Anal. At. Spectrom.*, 2000, **15**, 1143–1148.
38 A. Lorrain, D. P. Gillikin, Y.-M. Paulet, L. Chauvaud, A. L. Mercier, J. Navez and L. André, *Geology*, 2005, **33**, 965–968.
39 E. V. Putten, F. Dehairs, E. Keppens and W. Baeyens, *Geochim. Cosmochim. Acta*, 2000, **64**, 997–1011.
40 A. Katz, *Geochim. Cosmochim. Acta*, 1973, **37**, 1563–1586.